Human osteosarcoma cells respond to sorafenib chemotherapy by downregulation of the tumor progression factors *S100A4*, *CXCR4* and the oncogene *FOS*

INGRID WALTER[1,2], BIRGITT WOLFESBERGER[3], INGRID MILLER[4], GEORG MAIR[2], STEFANIE BURGER[2], BIRGIT GALLÈ[5] and RALF STEINBORN[2]

[1]Institute of Anatomy, Histology and Embryology, [2]VetOmics Core Facility, VetCore, [3]Clinic for Companion Animal Medicine, Unit for Internal Medicine, and [4]Institute for Medical Biochemistry, University of Veterinary Medicine, 1210 Vienna; [5]ZMF, Medical University, 8010 Graz, Austria

Received October 15, 2013; Accepted November 20, 2013

DOI: 10.3892/or.2013.2954

Abstract. Osteosarcoma is a rare but aggressive bone neoplasm in humans, which is commonly treated with surgery, classical chemotherapy and radiation. Sorafenib, an inhibitor of a number of kinases targeting the Raf/MEK/ERK pathway, is a promising new chemotherapeutic agent in human medicine that has been approved since 2006 for the therapy of renal cell carcinoma and since 2007 for the treatment of hepatocellular carcinoma. Here, we studied the antimetastatic potential of 4 μM of this multikinase inhibitor in a human osteosarcoma cell line. DNA microarray-based gene expression profiling detected 297 and 232 genes upregulated or downregulated at a threshold of >2-fold expression alteration ($P<0.05$) in the sorafenib-treated cells. Three genes (*CXCR4*, *FOS* and *S100A4*) that are involved in tumor progression were chosen for validation by quantitative PCR (qPCR) and protein expression analysis. The decrease in RNA expression detected by microarray profiling was confirmed by qPCR for all three genes ($P<0.01$). On the protein level, sorafenib-induced reduction of S100A4 was verified both by western blotting and immunohistochemistry. For CXCR4 and c-Fos, a reduced protein expression was shown by immunohistochemistry, for c-Fos also by immunoblotting. We conclude that sorafenib could serve as a potent chemotherapeutical agent by which to inhibit the metastatic progression of osteosarcomas.

Introduction

Osteosarcoma is the most common type of primary bone cancer in humans (1). The standard therapy regimen for high-grade osteosarcoma includes induction by neoadjuvant chemotherapy followed by surgical resection (mostly limb-sparing or rarely amputation), radiotherapy and adjuvant chemotherapy (2). Most of these neoplasms show a high-grade histopathology with the lung being the most common distant metastatic site (3). Invasion and metastasis are complex processes that involve cell-cell detachment, migration, extravasation, proliferation and angiogenesis. When distant metastases develop, the prognosis is poor. Proteins such as vascular endothelial growth factor (VEGF), stem cell factor receptor (c-kit) and platelet-derived growth factor (PDGF) have been found to be involved in osteosarcoma progression and metastasis formation (4-6). The serum concentration of VEGF was found to be significantly correlated with the survival time of humans with osteosarcoma (7). As a consequence of these observations, tyrosine kinase inhibitors were developed as potential anticancer drugs (8). Sorafenib (BAY 43-9906, Nexavar®, Bayer-Onyx), an oral small-molecule multikinase inhibitor, was developed by high-throughput screening of massive libraries of synthetic compounds primarily as a RAF (ras-activated factor) inhibitor blocking the RAF/MEK/ERK1/2 pathway. However, sorafenib was also shown to 'hit' several other targets such as vascular endothelial growth factor receptors (VEGFR-2 and 3), platelet derived growth factor receptor (PDGFR-β), c-kit receptor and fms-like tyrosine kinase 3 (flt-3) (9) and to modulate the innate and adaptive immune responses (10). For example, sorafenib inhibits JAK/STAT signaling by stimulating phosphatase SHP2 activity resulting in accelerated STAT3 dephosphorylation (11). Sorafenib antitumor therapy has been shown to involve an miRNA-based mechanism (12). Sorafenib can also alter the expression of proteins involved in metastasis such as the c-Fos proto-oncogene coded by the *FOS* gene (13), and combination therapy with an inhibitor of the chemokine receptor CXCR4 was found to result in enhanced antileukemic activity *in vitro* (14). In human osteosarcoma, sorafenib treatment blocks growth, angiogenesis and metastatic potential. Moreover, it dramatically reduced the tumor volume of osteosarcoma xenografts and lung metastasis in SCID mice (15). An antiproliferative effect of sorafenib in an osteosarcoma tumor cell line was shown to be due to the induction of apoptosis in a dose-dependent range (15,16).

Correspondence to: Professor Ingrid Walter, Institute of Anatomy, Histology and Embryology, University of Veterinary Medicine, Veterinaerplatz 1, 1210 Vienna, Austria
E-mail: ingrid.walter@vetmeduni.ac.at

Key words: S100A4, c-Fos, CXCR4, osteosarcoma cells, sorafenib, human

Here, we used DNA microarray expression analysis to study the effect of the multikinase inhibitor sorafenib on human osteosarcoma cells. Two key issues, identification of candidate targets of the antiproliferative and metastasis-inhibiting effect, and identification of putative therapeutic 'side-effects' using pathway enrichment analysis were addressed in the transcriptome profiling analysis. Three genes exhibiting altered RNA expression on the microarray and known to be highly involved in cancer progression were selected for qPCR validation and for protein expression analysis using western blotting and immunohistochemistry.

Materials and methods

Cell culture and treatment. Human osteosarcoma cells (ATCC CRL-1543™) were cultured in Dulbecco's modified Eagle's medium (Sigma Chemicals, Vienna, Austria) supplemented with 10% fetal calf serum, 1% penicillin/streptomycin, 1% L-glutamine and 0.25% Fungizone (Gibco, Paisley, UK). The cells were maintained in a humidified 5% CO_2 atmosphere at 37˚C. For the sorafenib treatment, experimental cells were passaged and seeded into 25-cm^2 flasks. After 24 h, the medium was removed and replaced with culture medium containing 4 μM sorafenib (Bayer, Vienna, Austria), dissolved in distilled water. For the experiment, the cells were incubated for 72 h with the sorafenib solution. Control cells were incubated with culture medium alone. The experiment was performed three times. After the incubation period, cells were washed in PBS and scratched from the culture flasks with a plastic cell scraper, pelleted and washed again in PBS. Further treatment was dependent on the use of the cells (RNA, protein) and is described in the respective section of Materials and methods.

DNA microarray analysis. Pelleted human osteosarcoma cells were washed twice in PBS and RNA was extracted using the RNeasy Plus Mini kit (Qiagen, Hilden, Germany) according to the manufacturer's protocol. Integrity of the RNA samples was controlled by capillary electrophoresis on the Agilent 2100 Bioanalyzer using the RNA 6000 Nano kit (Agilent Technologies, Foster City, CA, USA). Samples with an RNA integrity number (RIN) value of ≥9 were used for expression profiling. Human Genome Survey Arrays v2.0 (Applied Biosystems, Foster City, CA, USA) were used to determine the transcriptional profiles of sorafenib-treated and control cells. DIG-UTP-labeled cRNA was generated and linearly amplified from 2 μg total RNA using the Applied Biosystems Chemiluminescent RT-IVT Labeling kit v2.0 according to the manufacturer's protocol. Array hybridization, chemiluminescence detection, image acquisition and analysis were performed using Applied Biosystems Chemiluminescence Detection kit and Applied Biosystems 1700 Chemiluminescence Microarray Analyzer following the manufacturer's instructions. Briefly, each microarray was pre-hybridized in hybridization buffer with blocking reagent at 55˚C for 1 h. A total of 18 μg DIG-labeled cRNA targets were fragmented, mixed with internal control target and hybridized to the pre-hybridized microarrays in a volume of 1.5 ml at 55˚C for 16 h. After hybridization, the arrays were washed with hybridization wash buffer and chemiluminescence rinse buffer. Enhanced chemiluminescent signals were generated by incubating arrays with alkaline phosphatase-conjugated anti-digoxigenin antibody followed by incubation with chemiluminescence enhancing solution and a final addition of chemiluminescence substrate. Four images were collected for each microarray using the 1700 Chemiluminescent Microarray Analyzer. Images were autogridded and the chemiluminescent signals were quantified, corrected for background and spot and spatially normalized. Expression values of <10 were set to 10. Data were normalized to the 50th percentile (intra-array normalisation) and each gene was normalized to the median expression (inter-array normalisation). Data were pre-filtered based on the signal to noise ratio of >3-fold determined for all samples of the respective biological replicate group. Genes exhibiting normalized expression levels between 0.667- and 1.334-fold in at least four biological replicates (containing at least two replicates per group) were considered invariant and were removed from the deregulated gene list. The remaining data set was tested for differentially expressed genes using analysis of variance (ANOVA; GeneSpring Expression Analysis 7.3.1 tool; Agilent Technologies). Only significantly deregulated genes ($P<0.05$ in the parametric Welch t-test) were considered.

Gene set enrichment analysis. Significantly deregulated genes (n=522) were annotated to gene symbols of NCBI using the Database for Annotation, Visualization and Integrated Discovery (DAVID) v6.7 (17) and GeneMANIA (The GeneMANIA prediction server: Biological Network Integration for Gene Prioritisation and Predicting Gene Function) (18). The gene symbols were further converted to Entrez Gene of NCBI and Ensembl Gene identities employing the web-based conversion tool Clone/Gene ID Converter (19). Gene set enrichment analysis was performed by submitting all three identities in parallel to the pathway analytical applications DAVID and WEB-based Gene SeT AnaLysis Toolkit v2 (WebGestalt) (20) targeting the databases KEGG, Pathway Commons and WikiPathways. Cross-hybridising probes were excluded from the analysis. Genes that were not accepted by the latter databases were indirectly assigned to a pathway using functional association data of related genes with known gene ontology term assignations contained in GeneMANIA. These association data include protein and genetic interactions, pathways, co-expression, co-localisation and protein domain similarity.

Transcript quantification by qPCR. Exon boundaries and intron sizes of target and reference genes were determined using the mRNA-to-genomic alignment program Spidey of NCBI. Exons separated by an intron of >750 bp were targeted to design intron-flanking primers with Primer Express version 2.0 (Applied Biosystems). Amplicons were tested for secondary structure using the Mfold Web Server for Nucleic Acid folding and hybridization prediction (21) using 50 mM Na^+, 2 mM Mg^{2+} and a temperature of 60˚C as changes from default settings. The potential for primer dimerisation was assessed on the basis of the Gibbs free energy ΔG value calculated by the open source program NetPrimer (NetPrimer Biosoft International, Palo Alto, CA, USA). Primer/amplicon specificity was assessed by NCBI Primer-BLAST. Primer details are listed in Table I. Pellets of osteosarcoma cells were shock frozen and stored in liquid nitrogen until RNA isola-

Table I. Oligonucleotides for qPCR.

Gene	GenBank identity	Oligonucleotide sequence (5' to 3')
Genes of interest		
CXCR4, transcript variant 1[a]	NM_001008540.1	F: GCAGAGGAGTTAGCCAAGATGT R: CCCATCTTTTCCCATAGTGACTT P: FAM-TTGAAACCCTCAGCGTCTCAGTGCC-BHQ1
CXCR4, transcript variant 2	NM_003467.2	F: CAGCAGGTAGCAAAGTGACGC R: CCCATTTCCTGGTGTAGTTATCT P: FAM-CCTGAGTGCTCCAGTAGCCACCGC-BHQ1
FOS	NM_005252.3	F: TGGCGTTGTGAAGACCATGAC R: TATTCCTTTCCCTTCGGATTCTCCT P: not applied
S100A4, transcript variant 2	NM_019554.2	F: TCAAGCTCAACAAGTCAGAACTAAAGG R: GAAGTCCACCTCGTTGTCCC P: not applied
Reference genes		
OAZ1	NM_004152.2	F: GCACCATGCCGCTCCTAAG R: CATCAGGAGCACCACCGAG P: not applied
RPL41[b]	NM_001035267.1, NM_021104.1	F: AGAAAGATGAGGCAGAGGTCCA R: AATAGTCCAGAATGTCACAGGTCCA P: not applied

[a]Single-exon transcript, i.e. intron-flanking primer design was not possible. [b]Primers target exons 3 or 4 in *RPL41* transcript variants 1 (NM_001035267.1) or 2 (NM_021104.1), respectively. F, forward primer, R, reverse primer; P, dual-labeled hydrolysis probe. FAM, 6-carboxyfluorescein; BHQ1, Black Hole Quencher 1.

tion. Frozen cell pellets were lysed in a monophasic solution of phenol and guanidine thiocyanate (QIAzol lysis reagent; Qiagen) at 37˚C for 30 min applying continuous vortexing. Automated RNA purification was performed on the QIAcube using the miRNeasy Mini kit (Qiagen) followed by digestion with TURBO™ DNase (Life Technologies, Vienna, Austria) to remove contaminating DNA. RNA concentration was measured by UV spectrophotometry on the Hellma TrayCell (Hellma, Müllheim/Baden, Germany) in combination with the BioPhotometer 6131 (Eppendorf, Hamburg, Germany). Only samples with a RIN value of >7 were used for qPCR quantification.

cDNA primed with random RT primers was synthesized for 120 min at 37˚C using the High-Capacity reverse transcription kit (Applied Biosystems). For each cDNA duplicate 1000 ng RNA was reverse transcribed in a reaction volume of 20 μl. The 20 μl-qPCR consisted of 80 mM Tris-HCl (pH 9.4), 20 mM $(NH_4)_2SO_4$, 0.02% w/v Tween-20, 3 mM $MgCl_2$, 0.2 mM dNTPs, 200 nM of each primer, 0.4X EvaGreen DNA-binding dye (Biotium, Inc., Hayward, CA, USA), 1 unit of Hot FIREPol *Taq* DNA polymerase (Solis BioDyne, Tartu, Estonia) and 2 μl of a 1:10 dilution of the cDNA. The qPCR was conducted on the ABI PRISM 7900HT sequence detection system (Applied Biosystems) using a thermal protocol which consisted of an initial enzyme activation/denaturation step of 95˚C for 15 min followed by 45 amplification cycles (95˚C for 15 sec, 59˚C for 40 sec, 72˚C for 20 sec) and melting curve analysis between 65 and 95˚C. Amplicon specificity was evaluated based on the melting peak, i.e. the maximum in the negative derivative of the fluorescence to temperature (-d*F*/d*T*). Serial 8-fold dilutions of an equimolar pool of sample cDNAs amplified in duplicate were used to generate a standard curve. Reaction efficiencies (E) were calculated from the slope(s) of the standard curve using the formula $E = 10^{-1/s} - 1$. Specificity of a qPCR signal was concluded on the basis of a minus-RT control using a systematic error threshold of 1%. Calculation of gene expression ratios and evaluation of their statistical significance were performed with the relative expression software tool (REST) using the Pair Wise Fixed Reallocation Randomisation Test for statistical evaluation (22). Target gene expression was normalized with the reference genes *OAZ1* (23,24) and *RPL41* or with *OAZ1* alone (for transcript variants 1 and 2 of *CXCR4*). The geometric mean of both reference genes was used in case of *FOS* und *S100A4*. RT-qPCR data comply with the Minimum Information for Publication of Quantitative Real-Time PCR Experiments (MIQE) guidelines (25).

Western blotting. Cell pellets were lysed in low salt extraction buffer (10 mM Tris pH 7.5, 140 mM NaCl, 5 mM EDTA, 1 mM PMSF, 1 mM DTT) and protein concentration was determined (20 μg protein) according to the methods of Bradford (26). Appropriate amounts of samples were subjected to SDS-gel

Table II. Gene set enrichment analysis for genes showing altered RNA expression after sorafenib treatment and having a Gene Ontology term assignation.

Enriched pathway/network	P-value	Pathway database	Pathway analytical application used
Pathways in cancer	3.98E-09	KEGG	(20)
Proteogylcan syndecan-mediated signaling events	1.99E-08	Pathway Commons	(20)
ABC transporters	6.00E-07	KEGG	(17)
Syndecan-4-mediated signaling events	1.04E-06	Pathway Commons	(20)
Complement and coagulation cascades	2.40E-06	KEGG	(17)
Systemic lupus erythematosus	7.20E-06	KEGG	(17)
Cytokine-cytokine receptor interaction	1.27E-05	KEGG	(20)
MAPK signaling pathway	1.36E-05	KEGG	(20)
Chemokine signaling pathway	4.90E-05	KEGG	(17)
BMP receptor signaling	2.00E-04	Pathway Commons	(20)
Small cell lung cancer	2.00E-04	KEGG	(20)
GnRH signaling pathway	5.40E-04	KEGG	(17)
HIF-1-α transcription factor network	5.00E-04	Pathway Commons	(20)
Oocyte meiosis	7.50E-04	KEGG	(17)
Hypoxic and oxygen homeostasis regulation of HIF-1-α	1.90E-03	Pathway Commons	(20)
Myometrial relaxation and contraction pathways	2.30E-03	WikiPathways	(20)
Wnt signaling pathway	2.50E-03	KEGG	(20)
Leukocyte transendothelial migration	2.80E-03	KEGG	(20)
TNF receptor signaling pathway	3.00E-03	Pathway Commons	(20)
Melanogenesis	3.10E-03	KEGG	(20)
Estrogen signalling	3.50E-03	WikiPathways	(20)
NOD-like receptor signaling pathway	3.80E-03	KEGG	(20)
Glypican pathway	4.00E-03	Pathway Commons	(20)
Extrinsic pathway for apoptosis	5.80E-03	Pathway Commons	(20)
Death receptor signalling	5.80E-03	Pathway Commons	(20)
Long-term potentiation	6.00E-03	KEGG	(17)
Bladder cancer	6.20E-03	KEGG	(20)
Glypican 1 network	6.40E-03	Pathway Commons	(20)
Focal adhesion	6.50E-03	WikiPathways	(20)
Cell adhesion molecules (CAMs)	6.90E-03	KEGG	(20)
Progesterone-mediated oocyte maturation	9.40E-03	KEGG	(17)

Only pathways with P<0.001 are shown.

electrophoresis under reducing conditions on 140x140x1.5 mm gradient gels in a Hoefer SE-600 electrophoresis unit (Hoefer Scientific Instruments, San Francisco, CA, USA) according to Laemmli (27). After separation, protein bands were transferred onto appropriate membranes (nitrocellulose or PVDF; both from GE Healthcare Life Sciences, Munich, Germany) by semi-dry blotting in a Semi-Phor unit (Hoefer Scientific Instruments). Membranes were blocked for 2-4 h with 5% non-fat dry milk (Merck, Darmstadt, Germany) in TBS + 0.05% Tween-20, and further incubated in diluted antibodies anti-S100A4 (Dako, Glostrup, Denmark), anti-c-Fos (Synaptic Systems GmbH, Göttingen, Germany) and anti-CXCR4 (Abcam, Cambridge, UK or Santa Cruz Biotechnology, Santa Cruz, CA, USA) in 1-5% milk overnight at 4-6˚C followed by HRP-conjugate anti-rabbit IgG (0.1 μl Ab/cm^2; Sigma) for 2 h at room temperature. ECL or ECL Prime (both from GE Healthcare Life Sciences) was used to detect immunoreactive bands. Film was scanned on a Sharp JX-330 flatbed scanner and evaluated with the software Quantity One version 2.7 (PDI Inc., Huntington Station, NY, USA). The overall protein staining [fluorophore ruthenium(II)tris(bathophenanthroline disulfonate)] pattern was used as a loading control and for normalization. Human breast cancer cells (MDA-MB-231 and MCF-7) were used as positive control for the CXCR experiments. Molecular weight of proteins was predicted using the UniProtKB database (http://www.uniprot.org/uniprot/).

Immunohistochemistry. Human osteosarcoma cells were cultured on sterile glass coverslips and treated with sorafenib as described above. After the treatment, cells were washed in PBS and fixed in 4% buffered formaldehyde for 15 min, washed in distilled water and air dried. For immunostaining,

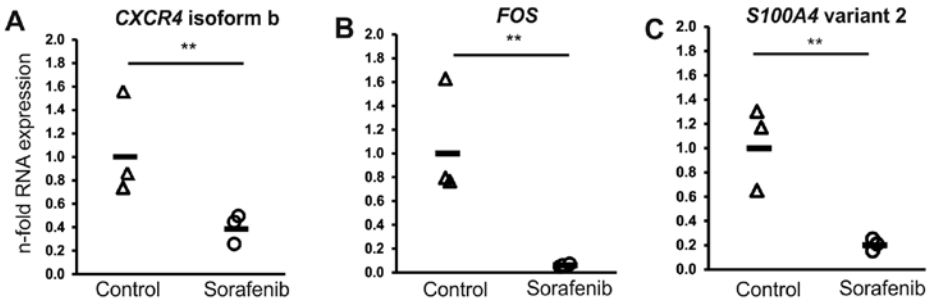

Figure 1. Transcript expression of (A) *CXCR4* isoform b, (B) *FOS* and (C) *S100A4* transcript variant 2 is downregulated in a human osteosarcoma cell line following treatment with 4 μM sorafenib. The horizontal bar designates the mean for the respective group. **P<0.01 determined by Pair Wise Fixed Reallocation Randomization Test©.

cells on coverslips were permeabilized with 0.2% Triton X-100 in PBS, rehydrated and endogenous peroxidases were eliminated by incubation in 0.06% H_2O_2 for 15 min. After blocking with 1.5% goat serum for 30 min, cells were incubated with primary polyclonal antibodies anti-S100A4 (dilution 1:100 in PBS; Thermo Fisher Scientific), anti-CXCR4 [dilution 1:100; Abcam (ab2090), Cambridge, UK] and c-Fos (dilution 1:300; Synaptic Systems GmbH) for 2 h at room temperature. For CXCR4-immunostaining antigen-retrieval by 2x 5-min heating in Tris-EDTA buffer pH 9.0, and for S100A4 and c-Fos boiling of the sections for 4x 5 min in citrate buffer (0.1 M) pH 6.0 was necessary. As secondary antibody an anti-rabbit poly-HRP antibody (BrightVision, Immunologic, Duiven, The Netherlands) was used. The signal was developed with DAB (Sigma) as a chromogen. Negative controls were incubated with PBS instead of the primary antibody while all the other steps were performed identically.

Results

DNA microarray analysis of RNA expression. The effect of the multikinase inhibitor sorafenib on a human osteosarcoma cell line was evaluated by DNA microarray analysis using three biological-technical replicates. In total, 1,847 genes were found to be differentially expressed between the sorafenib-treated cells and control cells at a significance level of P<0.05. At the threshold of >2-fold expression alteration, 297 and 232 genes were upregulated or downregulated by the treatment, respectively (data not shown). Two hundred and thirty-nine genes for which information on pathway/network assignation was available were analysed for gene set enrichment with the pathway analytical applications DAVID v6.7 and WebGestalt v2. The network termed pathways in cancer delivered the highest statistical support (Table II). Two hundred and ninety genes for which a pathway could not be assigned were analysed for enrichment using GeneMANIA. This database identifies other genes that are related to a set of input genes, using functional association data. GeneMANIA-based gene set enrichment analysis identified the extracellular matrix network as most affected (Table III).

Three downregulated genes which are involved in cancer progression and/or metastasis (*FOS*, *S100A4* and *CXCR4*) were selected for subsequent validation of RNA expression by RT-qPCR. The v-Fos FBJ (Finkel Biskis-Jinkis) murine osteosarcoma viral oncogene homolog (*FOS*) gene (0.1-fold change) was selected due to the highest significance of downregulation. The chemokine (C-X-C motif) receptor 4 (*CXCR4*) gene, and the S100 calcium binding protein A4 (*S100A4*) gene meeting the threshold of expression alteration of >2-fold (0.35- and 0.49-fold downregulation, respectively) were also included. The latter represented other downregulated members of the S100 protein family (*S100A3*, *S100A2*, *S100A16* and *S100A13*; expression changes of 0.28- to 0.49-fold).

Table III. GeneMANIA-based gene set enrichment analysis for genes showing altered RNA expression following sorafenib treatment and not having a pathway assignation.

Gene Ontology annotation	False discovery rate	Coverage[a]
Extracellular matrix	2.77E-07	19/180
Fibrillar collagen	3.62E-05	6/11
Collagen	9.25E-04	7/29
Collagen fibril organization	1.88E-03	6/21
Cellular response to type I interferon	2.49E-03	9/71
Skin development	5.45E-03	5/16
Proteinaceous extracellular matrix	5.45E-03	10/105
Extracellular matrix part	5.45E-03	8/61

Threshold for false discovery rate: <1.00E-02. [a]Number of deregulated genes/number of genes per Gene Ontology term.

Validation of RNA expression using qPCR. qPCR was used to verify the sorafenib-induced expression changes measured by microarray analysis for the chosen genes of interest. For all three genes (*FOS*, *S100A4* and *CXCR4*) selected, alteration of expression and its direction were confirmed (Fig. 1). In detail, for *FOS*, *S100A4* (transcript variant 2) and *CXCR4* (transcript variant 2; variant 1 not expressed; data not shown) a reduction in expression of 0.06-, 0.23- and 0.36-fold was determined, respectively.

Protein expression analysis. To elucidate protein expression changes of c-Fos, S100A4 and CXCR4 induced by sorafenib, we applied western blotting and immunohistochemical

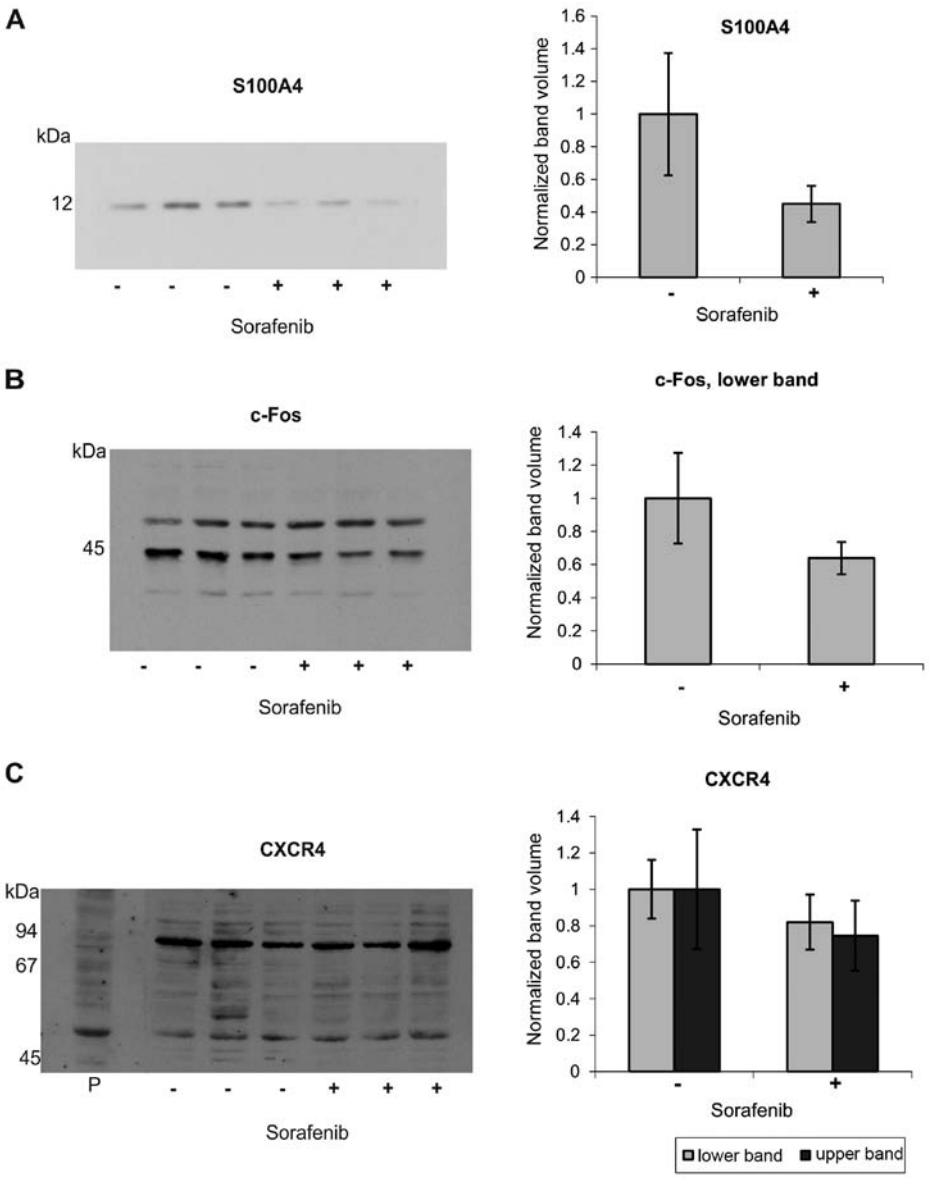

Figure 2. Protein expression analysis of (A) S100A4, (B) c-Fos and (C) CXCR4 using western blotting. (A) Sorafenib-treated human osteosarcoma cells (+) led to a marked reduction in S100A4 protein compared to control cells (-). (B) Two bands are visible after c-Fos antibody binding at 43 and 50 kDa. The upper band did not change, but the smaller protein was slightly reduced after sorafenib treatment. (C) The antibody against CXCR4 resulted in multiple bands; however, the intensity of the band at 50 kDa, which correlates to monomeric CXCR4, was moderately decreased after sorafenib treatment. P, positive control. Normalized band volumes are expressed in relation to the mean of the control group (three biological replicates).

methods. We found a marked reduction in the S100A4 band in the western blots in human osteosarcoma cells after sorafenib treatment (Fig. 2A). The antibody against c-Fos protein gave two prominent bands at ~43 and 50 kDa. Whereas the upper band was almost unaffected, the lower one showed a moderate reduction in human osteosarcoma cells after sorafenib treatment (Fig. 2B). CXCR4 proved to be difficult to detect with the commercially available antibodies tested. The antibody reactivities were low, needing higher signal amplification (ECL Prime), and resulted in multiple bands with a marked background staining for the Abcam antibody. Based on the positive control, the band at 50 kDa was assumed to correspond to monomeric CXCR4. This band was slightly reduced in intensity after sorafenib treatment (Fig. 2C). The antibody from Santa Cruz Biotechnology showed even higher background staining and only faint bands, already in controls, and was, therefore, excluded (data not shown). In parallel, immunohistochemical staining for S100A4 (Fig. 3A) and c-Fos (Fig. 3C) revealed a considerably reduced staining intensity between untreated and treated human osteosarcoma cells supporting the western blot data. Whereas the S100A4 protein was found in the cytoplasm of human osteosarcoma cells, c-Fos was restricted to the nucleus. CXCR4 immunostaining was predominantly noted in the cell membranes and the cytoplasm (Fig. 3B).

Discussion

Using DNA microarray expression analysis we showed that sorafenib affects the transcription profile of a series of genes in the human osteosarcoma cell line CRL-1543. From the set of downregulated genes, *S100A4*, *FOS* and *CXCR4*, playing a major role in tumor progression and metastasis were studied in detail.

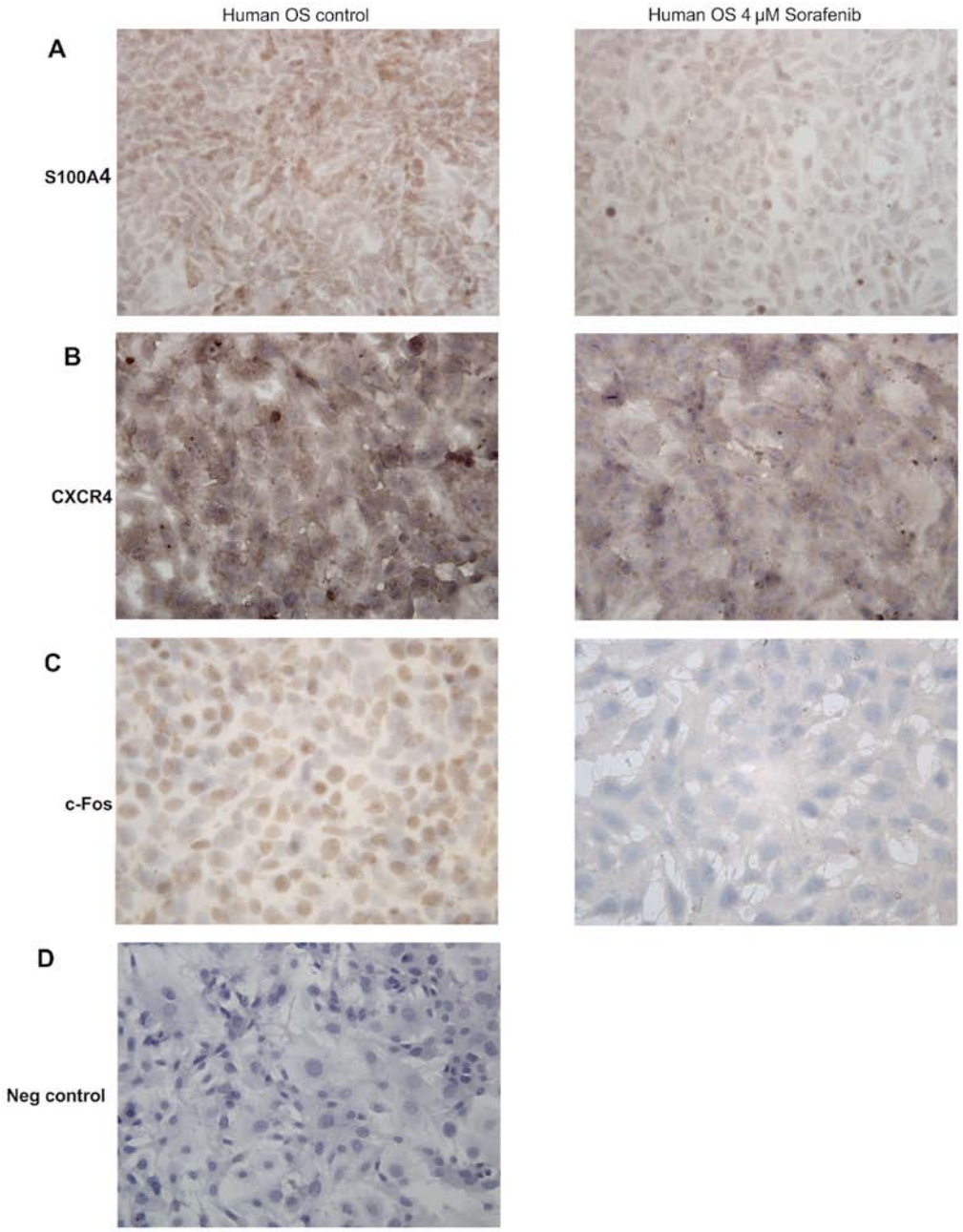

Figure 3. Immunohistochemical staining of human osteosarcoma cells for (A) S100A4, (B) CXCR4 and (C) c-Fos with and without 4 μM sorafenib treatment. Note the decreased staining intensity of these proteins in sorafenib-treated human osteosarcoma cells. (D) Negative control. OS, osterosarcoma.

S100A4 expression. S100A4, alternatively termed metastasin, represents a member of the family of calcium-binding proteins. S100A4 is a calcium-binding protein and is localized in the nucleus, cytoplasm and extracellular space and possesses a wide range of biological functions such as regulation of angiogenesis, cell survival, motility and invasion (28). S100A4 has no enzymatic activity and exerts its function mainly through interaction with other proteins. It has been shown to interact with a number of cytoskeleton-associated proteins including non-muscle myosin, actin, non-muscle tropomyosin and tubulin. S100A4 was the first protein of the S100 protein family shown to promote lung metastases in a model system of breast cancer (29). S100A4 is a well-established marker of metastatic disease, but the exact mechanisms responsible for the metastasis-promoting effects of this calcium-binding protein are less well defined (28). The basic approach to cancer therapy is through the inhibition of cell proliferation and disruption of the cell division machinery. S100A4 is capable of regulating cell cycle progression and influencing cytoskeletal dynamics and remodelling of the extracellular matrix and in this way affects invasion and metastasis (30). Inhibition of S100A4 results in a decrease in cell growth (31), a known effect of sorafenib on tumor cells *in vitro* (16). S100A4 influences angiogenesis and vascular density (32). This is an important finding since a strategy is being developed to employ tyrosine kinase inhibitors specifically to target the process of angiogenesis. Moreover, S100A4 downregulates the expression of the angiogenesis-inhibitor thrombospondin (33).

VEGF, a well-known factor of angiogenesis stimulation, is a downstream target of S100A4 (30). S100A4 plays a key role in the metastatic behavior of tumor cells; therefore, it is a promising molecular target for cancer therapy (30). *S100A4* expression was found to occur in parallel with cancer metastasis (30), was the most significant predictor of patient survival in a breast cancer study (34), and has a high prognostic significance in several other tumors (35,36). Highly malignant breast cancer cells were not able to metastasize in an S100A4 knockout mouse model (37). S100A4 is secreted by normal and neoplastic cells *in vitro* and *in vivo* (28). It regulates matrix-metalloproteinase-2 (MMP-2) activity in human osteosarcoma cells (38) and acts as a potent stimulator of angiogenesis (32). Inhibition of S100A4 expression by RNA interference was found to completely prevent metastasis formation in a mouse thyroid carcinoma model (31) and reduced invasiveness and proliferation of the human osteosarcoma cell line MG-63 (39). S100A4 was found to be expressed in >70% of clinical osteosarcoma samples and in the osteosarcoma cell lines MG-63 and U-2OS, but not in benign osteochondroma (39) supporting the significance of S100A4 as a marker of malignancy.

Here, *S100A4* was found to be expressed at the RNA and protein levels. Transcript variant 2 of *S100A4* as detected by RT-qPCR (Fig. 1) has been previously described (40). However, the significance of the two S100A4 transcripts with respect to gene activity in cancer progression remains unclear (41). In conclusion, as S100A4 is present in most osteosarcomas (39), we suggest that inhibition of the S100A4 protein may be a promising approach to reduce the malignant potential of osteosarcomas in patients.

FOS expression. c-Fos encoded by the *FOS* gene was initially identified as an oncoprotein of the Finkel Biskis-Jinkis osteosarcoma virus (42). Heterodimers are formed by Fos family members with members of other protein families such as JUN or ATF (activation transcription factor) to compose the AP-1 (activator protein) proteins. Reports on the action of AP-proteins in tumor formation and progression are contradictory. On the one hand, tumor-suppressor activity of AP-1 transcription factors was found (43), on the other hand, they were identified to play a major role in gene regulation during cell invasion, proliferation and malignant transformation. Transgenic mice overexpressing the c-Fos proto-oncogene develop osteosarcomas (44). Therefore, a reduction in *FOS* expression should lead to a decrease in the metastatic potential of a tumor and was for this reason chosen as a gene of interest.

The present study showed a decrease in *FOS* mRNA expression in human osteosarcoma cells following sorafenib treatment (Fig. 1). Evaluation of protein expression by western blot analysis showed two bands, at ~43 and 50 kDa. The lower one was downregulated by sorafenib treatment to approximately two-thirds compared to the controls (Fig. 2) and is in accordance with the theoretical molecular weight predicted for c-Fos (40.7 kDa; UniProtKB, http://www.uniprot.org/uniprot/P01100, version 74 from May 1, 2013). The band with the larger molecular weight could belong to FosB, another member of the Fos family of nuclear oncogenes. This family includes the highly homologous proteins c-Fos, FosB, Fos-related antigen 1 (FRA1) and Fos-related antigen 2 (FRA2) (45). It seems likely that their high homology is responsible for the cross-reactivity of the c-Fos antibody used in the present study. Downregulation of c-Fos by sorafenib is an important finding as Fos is overexpressed in the majority of human osteosarcomas (45) with high expression levels of c-Fos (47). Overexpression of c-Fos, a transcription factor of the activator protein-1 (AP-1) family, is involved in osteosarcoma formation in mice (44,48). The AP-1 complex can form many different homodimers and heterodimers that determine the genes that are regulated (43). c-Fos regulates the expression of MMPs (49) that play a role in tumor cell migration and therefore, in the process of metastasis. AP-1 regulates the genes that are required for tumor metastasis such as Ezrin, FasL and EGFR. In advanced tumors, c-Fos/AP-1 complexes were shown to induce the expression of genes that are involved in angiogenesis and tumor invasiveness (43). Blocking c-Fos expression by small interfering RNA (siRNA) in human colon carcinoma cells was found to lead to a significant reduction in transforming growth factor β1 (TGFβ1) and as a consequence reduced tumor cell growth (50). Strong *FOS* expression is also highly correlated with poor response to chemotherapy (51); therefore, it is an important therapeutic and prognostic biomarker.

CXCR4 expression. CXCR4 has been reported to play a major role in the metastatic process in osteosarcomas (52,53). It was suggested to be a useful prognostic factor and a predictor of metastatic development in osteosarcoma based on its correlation with the metastatic behavior of osteosarcoma, and its common expression in high-grade osteosarcoma samples at a level inversely correlated to overall survival (53). Moreover, tumors expressing both CXCR4 and VEGF were found to have worse overall survival rates compared with the survival of patients with tumors that lacked one of these factors (54). Contradictory results were obtained for the role of CXCR4 in human osteosarcoma in which CXCR4/CXCL12 was correlated with a better long-term outcome and a lower prevalence of metastases (55). However, in an osteosarcoma mouse model, inhibition of the CXCR4 site resulted in the elimination of lung metastases (56), and antagonists of CXCR4 such as neutralizing antibodies were also markedly found to reduce metastasis (57,58). Silencing of *CXCR4* mRNA impaired invasion of breast cancer cells in a Matrigel invasion assay and inhibited breast cancer metastasis in an animal model (59) underlining the importance of this factor in tumor malignancy. These partly contradictory findings might be associated with the manifold isoforms and variants of CXCR4 that occur.

Two splice variants of *CXCR4* have been described (http://www.uniprot.org/uniprot/P61073), and only one of these was found to be expressed by qPCR in our model (Fig. 1). The diverging results obtained for *CXCR4* by expression analyses after mRNA and protein levels (Figs. 1 and 2) could be due to a concomitant sorafenib impairment of miRNA-mediated post-transcriptional regulation (12). The size difference between the two *CXCR4* splice variants is <1 kDa and thus too small to be detectable at the protein level by SDS-PAGE. In addition, the antibodies tested in the present study gave multiple bands with our samples. The presumptive CXCR4 band was confirmed by comparison with a human breast cancer cell line and was slightly decreased in intensity after sorafenib treatment. Moreover, other studies report additional bands in the western blots of CXCR4, which are attributed e.g. to dimer-

ization, glycosylation, ubiquitination or heterogeneity of the molecule (60-62). This might explain the similar regulation of the second main band.

Therapeutic perspectives. The reduction of the three molecular targets following sorafenib treatment found in our *in vitro* study is a positive signal for the application of this drug in osteosarcoma disease, although cell culture might not reflect the *in vivo* responsiveness and complexity and occurrence of possible side-effects. A phase II clinical trial with sorafenib in relapsed and unresectable osteosarcoma demonstrated clinical effects in the form of partial responses, minor responses and stable diseases with a median progression-free survival of 4 months and an overall survival time of 7 months (63).

A detailed analysis of metastasis-associated factors in different types of osteosarcoma can help to identify ubiquitous targets for a more focused anticancer therapy. Molecules such as receptors, ion channels and enzymes can be targeted by chemical-library screening and natural-product chemistry, the random search through millions of chemical compounds, or by synthesis of a chemical entity that is tailored to fit its target, i.e. structure-based drug design. Transition-state analogue design, a more recent approach to drug design, by contrast, is limited to enzyme targets. It mimics the normal reactant's transition-state geometry to facilitate tighter binding of a transition-state analogue to its parent enzyme compared to the normal reactant (64) preventing the normal reactants from binding and resulting in enzyme inhibition. The strength of binding of the analogue considerably reduces the amounts of a drug needed to be delivered to the target enzyme. The long-lasting effect of the analogue (65) would in theory minimize therapeutic side-effects.

Acknowledgements

The authors thank Christian Gülly and Slave Trajanoski for their support.

References

1. Kansara M and Thomas DM: Molecular pathogenesis of osteosarcoma. DNA Cell Biol 26: 1-18, 2007.
2. Ta HT, Dass CR, Choong PF and Dunstan DE: Osteosarcoma treatment: state of the art. Cancer Metastasis Rev 28: 247-263, 2009.
3. Withrow SJ, Powers BE, Straw RC and Wilkins RM: Comparative aspects of osteosarcoma. Dog versus man. Clin Orthop Relat Res 270: 159-168, 1991.
4. Kaya M, Wada T, Akatsuka T, Kawaguchi S, Nagoya S, Shindoh M, Higashino F, Mezawa F, Okada F and Ishii S: Vascular endothelial growth factor expression in untreated osteosarcoma is predictive of pulmonary metastasis and poor prognosis. Clin Cancer Res 6: 572-577, 2000.
5. Smithey BE, Pappo AS and Hill DA: C-kit expression in pediatric solid tumours: a comparative immunohistochemical study. Am J Surg Pathol 26: 486-492, 2002.
6. McGary EC, Weber K, Mills L, Doucet M, Lewis V, Lev DC, Fidler IJ and Bar-Eli M: Inhibition of platelet-derived growth factor-mediated proliferation of osteosarcoma cells by the novel tyrosine kinase inhibitor STI571. Clin Cancer Res 8: 3584-3591, 2002.
7. Kaya M, Wada T, Nagoya S, Sasaki M, Matsumura T and Yamashita T: The level of vascular endothelial growth factor as a predictor of a poor prognosis in osteosarcoma. J Bone Joint Surg Br 91: 784-788, 2009.
8. Steeghs N, Nortier JW and Gelderblom H: Small molecule tyrosine kinase inhibitors in the treatment of solid tumours: an update of recent developments. Ann Surg Oncol 14: 942-953, 2007.
9. Wilhelm SM, Carter C, Tang L, *et al*: BAY 43-9006 exhibits broad spectrum oral antitumour activity and targets the RAF/MEK/ERK pathway and receptor tyrosine kinases involved in tumour progression and angiogenesis. Cancer Res 64: 7099-7109, 2004.
10. Mulder SF, Jacobs JF, Olde Nordkamp MA, *et al*: Cancer patients treated with sunitinib or sorafenib have sufficient antibody and cellular immune responses to warrant influenza vaccination. Clin Cancer Res 17: 4541-4549, 2011.
11. Blechacz BR, Smoot RL, Bronk SF, Werneburg NW, Sirica AE and Gores GJ: Sorafenib inhibits signal transducer and activator of transcription-3 signaling in cholangiocarcinoma cells by activating the phosphatase shatterproof 2. Hepatology 50: 1861-1870, 2009.
12. Zhou C, Liu J, Li Y, Liu L, Zhang X, Ma CY, Hua SC, Yang M and Yuan Q: microRNA-1274a, a modulator of sorafenib induced a disintegrin and metalloproteinase 9 (ADAM9) down-regulation in hepatocellular carcinoma. FEBS Lett 585: 1828-1834, 2011.
13. Ramakrishnan V, Timm M, Haug JL, Kimlinger TK, Wellik LE, Witzig TE, Rajkumar SV, Adjei AA and Kumar S: Sorafenib, a dual Raf kinase/vascular endothelial growth factor receptor inhibitor has significant anti-myeloma activity and synergizes with common anti-myeloma drugs. Oncogene 29: 1190-1202, 2010.
14. Zeng Z, Shi YX, Samudio IJ, *et al*: Targeting the leukemia microenvironment by CXCR4 inhibition overcomes resistance to kinase inhibitors and chemotherapy in AML. Blood 113: 6215-6224, 2009.
15. Pignochino Y, Grignani G, Cavalloni G, *et al*: Sorafenib blocks tumour growth, angiogenesis and metastatic potential in preclinical models of osteosarcoma through a mechanism potentially involving the inhibition of ERK1/2, MCL-1 and ezrin pathways. Mol Cancer 8: 118, 2009.
16. Wolfesberger B, Tonar Z, Gerner W, Skalicky M, Heiduschka G, Egerbacher M, Thalhammer JG and Walter I: The tyrosine kinase inhibitor sorafenib decreases cell number and induces apoptosis in a canine osteosarcoma cell line. Res Vet Sci 88: 94-100, 2010.
17. Huang da W, Sherman BT and Lempicki RA: Systematic and integrative analysis of large gene lists using DAVID bioinformatics resources. Nat Protoc 4: 44-57, 2009.
18. Warde-Farley D, Donaldson SL, Comes O, *et al*: The GeneMANIA prediction server: biological network integration for gene prioritization and predicting gene function. Nucleic Acids Res 38: W214-W220, 2010.
19. Alibes A, Yankilevich P, Canada A and Diaz-Uriarte R: IDconverter and IDClight: conversion and annotation of gene and protein IDs. BMC Bioinformatics 8: 9, 2007.
20. Duncan D, Prodduturi N and Zhang B: WebGestalt2: an updated and expanded version of the Web-based Gene Set Analysis Toolkit. BMC Bioinformatics 11: P10, 2010.
21. Zuker M: Mfold web server for nucleic acid folding and hybridization prediction. Nucleic Acids Res 31: 3406-3415, 2003.
22. Pfaffl MW, Horgan GW and Dempfle L: Relative expression software tool (REST) for group-wise comparison and statistical analysis of relative expression results in real-time PCR. Nucleic Acids Res 30: e36, 2002.
23. de Jonge HJ, Fehrmann RS, de Bont ES, Hofstra RM, Gerbens F, Kamps WA, de Vries EG, van der Zee AG, te Meerman GJ and ter Elst A: Evidence based selection of housekeeping genes. PLoS One 2: e898, 2007.
24. Kwon MJ, Oh E, Lee S, *et al*: Identification of novel reference genes using multiplatform expression data and their validation for quantitative gene expression analysis. PLoS One 4: e6162, 2009.
25. Bustin SA, Benes V, Garson JA, *et al*: The MIQE guidelines: Minimum Information for Publication of Quantitative Real-time PCR experiments. Clin Chem 55: 611-622, 2009.
26. Bradford MM: A rapid and sensitive method for the quantitation of microgram quantities of protein utilizing the principle of protein-dye binding. Anal Biochem 72: 248-254, 1976.
27. Laemmli UK: Cleavage of structural proteins during the assembly of the head of bacteriophage T4. Nature 227: 680-685, 1970.
28. Boye K and Maelandsmo GM: S100A4 and metastasis: a small actor playing many roles. Am J Pathol 176: 528-535, 2010.

29. Jenkinson SR, Barraclough R, West CR and Rudland PS: S100A4 regulates cell motility and invasion in an *in vitro* model for breast cancer metastasis. Br J Cancer 90: 253-262, 2004.
30. Sherbet GV: Metastasis promoter S100A4 is a potentially valuable molecular target for cancer therapy. Cancer Lett 280: 15-30, 2009.
31. Shi Y, Zou M, Collison K, Baitei EY, Al-Makhalafi Z, Farid NR and Al-Mohanna FA: Ribonucleic acid interference targeting S100A4 (Mts1) suppresses tumour growth and metastasis of anaplastic thyroid carcinoma in a mouse model. J Clin Endocrinol Metab 91: 2373-2379, 2006.
32. Ambartsumian N, Klingelhofer J, Grigorian M, *et al*: The metastasis-associated Mts1(S100A4) protein could act as an angiogenic factor. Oncogene 20: 4685-4695, 2001.
33. Schmidt-Hansen B, Klingelhofer J, Grum-Schwensen B, Christensen A, Andresen S, Kruse C, Hansen T, Ambartsumian N, Lukanidin E and Grigorian M: Functional significance of metastasis-inducing S100A4(Mts1) in tumour-stroma interplay. J Biol Chem 279: 24498-24504, 2004.
34. Rudland PS, Platt-Higgins A, Renshaw C, West CR, Winstanley JH, Robertson L and Barraclough R: Prognostic significance of the metastasis-inducing protein S100A4 (p9Ka) in human breast cancer. Cancer Res 60: 1595-1603, 2000.
35. Lee WY, Su WC, Lin PW, Guo HR, Chang TW and Chen HH: Expression of S100A4 and Met: potential predictors for metastasis and survival in early-stage breast cancer. Oncology 66: 429-438, 2004.
36. Wang YY, Ye ZY, Zhao ZS, Tao HQ and Chu YQ: High-level expression of S100A4 correlates with lymph node metastasis and poor prognosis in patients with gastric cancer. Ann Surg Oncol 17: 89-97, 2010.
37. Grum-Schwensen B, Klingelhofer J, Berg CH, El-Naaman C, Grigorian M, Lukanidin E and Ambartsumian N: Suppression of tumour development and metastasis formation in mice lacking the *S100A4 (mts1)* gene. Cancer Res 65: 3772-3780, 2005.
38. Mathisen B, Lindstad RI, Hansen J, El-Gewely SA, Maelandsmo GM, Hovig E, Fodstad O, Loennechen T and Winberg JO: S100A4 regulates membrane induced activation of matrix metalloproteinase-2 in osteosarcoma cells. Clin Exp Metastasis 20: 701-711, 2003.
39. Ma X, Yang Y, Wang Y, An G and Lv G: Small interfering RNA-directed knockdown of S100A4 decreases proliferation and invasiveness of osteosarcoma cells. Cancer Lett 299: 171-181, 2010.
40. Ambartsumian N, Tarabykina S, Grigorian M, Tulchinsky E, Hulgaard E, Georgiev G and Lukanidin E: Characterization of two splice variants of metastasis-associated human *mts1* gene. Gene 159: 125-130, 1995.
41. Mazzucchelli L: Protein S100A4: too long overlooked by pathologists? Am J Pathol 160: 7-13, 2002.
42. Durchdewald M, Angel P and Hess J: The transcription factor Fos: a Janus-type regulator in health and disease. Histol Histopathol 24: 1451-1461, 2009.
43. Eferl R and Wagner EF: AP-1: a double-edged sword in tumourigenesis. Nat Rev Cancer 3: 859-868, 2003.
44. Wang ZQ, Liang J, Schellander K, Wagner EF and Grigoriadis AE: *c-fos*-induced osteosarcoma formation in transgenic mice: cooperativity with *c-jun* and the role of endogenous *c-fos*. Cancer Res 55: 6244-6251, 1995.
45. Dobrazanski P, Noguchi T, Kovary K, Rizzo CA, Lazo PS and Bravo R: Both products of the fosB gene, FosB and its short form, FosB/SF, are transcriptional activators in fibroblasts. Mol Cell Biol 11: 5470-5478, 1991.
46. Wu JX, Carpenter PM, Gresens C, Keh R, Niman H, Morris JW and Mercola D: The proto oncogene c-fos is over-expressed in the majority of human osteosarcomas. Oncogene 5: 989-1000, 1990.
47. Franchi A, Calzolari A and Zampi G: Immunohistochemical detection of c-fos and c-jun expression in osseous and cartilaginous tumours of the skeleton. Virchows Arch 432: 515-519, 1998.
48. Ruther U, Komitowski D, Schubert FR and Wagner EF: c-fos expression induces bone tumours in transgenic mice. Oncogene 4: 861-865, 1989.
49. Hu E, Mueller E, Oliviero S, Papaioannou VE, Johnson R and Spiegelman BM: Targeted disruption of the c-fos gene demonstrates c-fos-dependent and -independent pathways for gene expression stimulated by growth factors or oncogenes. EMBO J 13: 3094-3103, 1994.
50. Pandey MK, Liu G, Cooper TK and Mulder KM: Knockdown of c-Fos suppresses the growth of human colon carcinoma cells in athymic mice. Int J Cancer 130: 213-222, 2012.
51. Kakar S, Mihalov M, Chachlani NA, Ghosh L and Johnstone H: Correlation of c-fos, p53, and PCNA expression with treatment outcome in osteosarcoma. J Surg Oncol 73: 125-126, 2000.
52. Clark JC, Dass CR and Choong PF: A review of clinical and molecular prognostic factors in osteosarcoma. J Cancer Res Clin Oncol 134: 281-297, 2008.
53. Laverdiere C, Hoang BH, Yang R, Sowers R, Qin J, Meyers PA, Huvos AG, Healey JH and Gorlick R: Messenger RNA expression levels of CXCR4 correlate with metastatic behavior and outcome in patients with osteosarcoma. Clin Cancer Res 11: 2561-2567, 2005.
54. Lin F, Zheng SE, Shen Z, Tang LN, Chen P, Sun YJ, Zhao H and Yao Y: Relationships between levels of CXCR4 and VEGF and blood-borne metastasis and survival in patients with osteosarcoma. Med Oncol 28: 649-653, 2011.
55. Baumhoer D, Smida J, Zillmer S, Rosemann M, Atkinson MJ, Nelson PJ, Jundt G, Luettichau IV and Nathrath M: Strong expression of CXCL12 is associated with a favorable outcome in osteosarcoma. Mod Pathol 25: 522-528, 2012.
56. Perissinotto E, Cavalloni G, Leone F, *et al*: Involvement of chemokine receptor 4/stromal cell-derived factor 1 system during osteosarcoma tumour progression. Clin Cancer Res 11: 490-497, 2005.
57. Liang Z, Wu T, Lou H, Yu X, Taichman RS, Lau SK, Nie S, Umbreit J and Shim H: Inhibition of breast cancer metastasis by selective synthetic polypeptide against CXCR4. Cancer Res 64: 4302-4308, 2004.
58. Mori T, Doi R, Koizumi M, *et al*: CXCR4 antagonist inhibits stromal cell-derived factor 1-induced migration and invasion of human pancreatic cancer. Mol Cancer Ther 3: 29-37, 2004.
59. Liang Z, Yoon Y, Votaw J, Goodman MM, Williams L and Shim H: Silencing of CXCR4 blocks breast cancer metastasis. Cancer Res 65: 967-971, 2005.
60. Carlisle AJ, Lyttle CA, Carlisle RY and Maris JM: CXCR4 expression heterogeneity in neuroblastoma cells due to ligand-independent regulation. Mol Cancer 8: 126, 2009.
61. Lapham CK, Romantseva T, Petricoin E, King LR, Manischewitz J, Zaitseva MB and Golding H: CXCR4 heterogeneity in primary cells: possible role of ubiquitination. J Leukoc Biol 72: 1206-1214, 2002.
62. Sloane AJ, Raso V, Dimitrov DS, *et al*: Marked structural and functional heterogeneity in CXCR4: separation of HIV-1 and SDF-1α responses. Immunol Cell Biol 83: 129-143, 2005.
63. Grignani G, Palmerini E, Dileo P, *et al*: A phase II trial of sorafenib in relapsed and unresectable high-grade osteosarcoma after failure of standard multimodal therapy: an Italian Sarcoma Group study. Ann Oncol 23: 508-516, 2012.
64. Ho MC, Shi W, Rinaldo-Matthis A, Tyler PC, Evans GB, Clinch K, Almo SC and Schramm VL: Four generations of transition-state analogues for human purine nucleoside phosphorylase. Proc Natl Acad Sci USA 107: 4805-4812, 2010.
65. Lewandowicz A, Tyler PC, Evans GB, Furneaux RH and Schramm VL: Achieving the ultimate physiological goal in transition state analogue inhibitors for purine nucleoside phosphorylase. J Biol Chem 278: 31465-31468, 2003.